

Parallel Acceleration of Fixed Complexity Sphere Decoder for Large MIMO Uplink System based on GPU

Tianpei Chen, Harry Leib

Department of Electrical and Computer Engineering

McGill University

Montreal, Quebec

October 17, 2014

Abstract

The large MIMO system which is a scaling up of conventional MIMO systems with several hundreds of antennas at the base station serving several tens of terminals at the same time, which is thought to be a big idea for the next generation wireless communication system. However the detection of the large MIMO system

acquires a long time to get optimum or sub-optimum solutions, In order to accelerate the real-time decoder for large MIMO system, in this paper we present General Purpose Graphic Processing Units (GPGPU) implementation of Fixed Complexity Sphere Decoder (FCSD) for the large scale MIMO system based on the dominant propriety framework of GPGPU-Computed Unified Device Architecture (CUDA). The simulation shows a up to nearly 5 times acceleration for 32×32 array of whole application CPU version, furthermore, the proposed CUDA-FCSD algorithm shows a increasing speedup performance for a increasing array size.

1 Introduction

The common challenge that all the researchers, engineers and industrial companies are now facing in wireless communication area is the sharp contrast between the increasing demand of the mobile network speed for the transmission of rich media content and better QoS (quality of service) and the limited bandwidth of the radio frequency spectrum and a complex space time varying wireless environment, moreover in foreseeable future this demand will continue grow. Multiple Input Multiple Output (MIMO) has become a very promising technology that can help to solve this problem, the core idea of MIMO is to use multiple antennas both at the transmitting end and receiving end, the spatial domain sampled signal can be combined to provide parallel data pipes so that

it can provide array gain, spatial diversity gain, spatial multiplexing gain, and interference reduction [1]. LTE standard support up to 8 antennas at the base station [2], The large scale MIMO (also named massive MIMO) is a system with hundreds of low-power low-price antennas collocated at the base station and serving several tens of terminals at the same time [3], originated from multiuser MIMO (MU-MIMO) [4]. Large scale MIMO will inherit and enhance all the advantages of conventional MIMO (array gain, spatial diversity gain, spatial multiplexing gain and interference reduction), as well as reduction of latency, improvement of the whole system robustness. As a classical list based decoder for MIMO system, Sphere decoder (SD) can reach the optimum diversity gain as maximum likelihood (ML) detection with a dramatic complexity reduction [5] [6], however, there are two major problems of this decoder is the varied complexity with signal to noise ratio and sequential nature, which is contradictory with the requirement of a constant data processing throughput and parallel implementation for practical system. Fixed Complexity Sphere Decoder (FCSD), overcomes this two disadvantage of the SD by searching the solution along the fixed number independent multiple paths [7]. GPGPU (General purpose Graphic processing Units Computing) has become a big idea in the industry and research of a variety of areas that needs massive data analysis and computation such as computer vision [8], computer games [9], signal processing [10] [11] and finance [12]. Comparing to CPU, The GPU has been designed as computational in-

tensive, with most of the hardware resource be allocated for data processing and parallel computation rather than caching and flow control. In recent years GPU has reached huge advantages in data processing speed over CPU [13]. CUDA (Computed unified Device Architecture) is a programming model for GPGPU that proposed by Nvidia which has becoming the dominant proprietary framework for GPGPU programming, it is based on popular programming languages(C, C++, java, python, Fortran, Direct Compute) so that the application developers in different areas do not need to learn a new programming language or get to know the hardware details. The core essence of the CUDA is the Single Instruction Multiple Threads (SIMT) programming model, enables GPU can accelerate a lot of applications with the large dataset by implementing parallel data processing of complex computations. CUDA has become a parallel computing platform for wide community of different application developers in different areas.

2 MIMO System Model

We consider a complex uncoded spatial multiplexing MIMO system with N_r receive antennas and N_t transmit antennas, $N_r \geq N_t$, in the flat fading channel the corresponding discrete time model is given:

$$y = \mathbf{H}s + n \tag{1}$$

$s \in \mathbb{C}^{N_t \times 1}$ is the transmit symbol vector, the symbol in s are mutually independent and taken from the signal constellation \mathbb{O} (BPSK, QPSK, M-QAM), M is the signal constellation size, all the transmit symbol vectors forms a N_t -dimensional signal constellation \mathbb{O}^{N_t} . $\varepsilon[ss^H] = I_{N_t} E_s$, E_s denotes the symbol average energy where ε denotes the mean operation. $y \in \mathbb{C}^{N_r \times 1}$ is the receive symbol vector, $\mathbf{H} \in \mathbb{C}^{N_r \times N_t}$ denotes the Rayleigh fading channel propagation matrix with independent identity distributed(i.i.d) circularly symmetric complex Gaussian zero mean elements of unit variance, $n \in \mathbb{C}^{N_r \times 1}$ is the additive white Gaussian noise (AWGN) samples with zero mean elements of variance $\varepsilon[nn^H] = I_{N_r} N_0$, N_0 denotes the average noise energy, $\frac{E_s}{N_0}$ denotes the signal to noise ratio (SNR).

Assume we have the perfect channel state information (CSI) \mathbf{H} , receive symbol vector y , and we had already known the SNR, the task of decoder for MIMO system is to estimate s in 1 based on CSI and received signal.

3 CUDA GPU Architecture and Programming Model

CUDA programming model is the C programming extension, with special defined syntax and structure, CUDA divide the CPU and GPU as host and device, the serial code executes on the host (CPU) side and parallel data processing is performed on the device

(GPU) side, which is defined as heterogeneous programming model. The code executes on the device side is defined as *kernel* function, which is a single instruction invoked at host side but with a massive parallel data processing threads execution on the device (SIMT), This programming architecture is akin to Single Instruction Multiple Data (SIMD), however unlike the SIMD vectoring machines, SIMT can branching the behavior of each threads so that reach thread-level parallelism, thread is the basic programming unit of CUDA, a block of cooperative threads form a thread block, in one block all the threads can share a memory called shared memory that all the threads in the block have the access to this patch of memory, the GPU use massive number of threads to hide the long latency of global memory instead of using large cache as CPU, Another function of the thread block is all the thread execute in one block can synchronize their action. The warp is the basic schedule unit with a constant number of threads (for current version of CUDA device, the warp size is 32), when one warp are waiting for data loading the other warps just begin to execute. In a word CPU cores are designed to minimize latency for each thread at a time , whereas GPUs are designed to handle a large number of concurrent, lightweight threads in order to maximize throughput. Blocks are grouped into a one-dimensional, two-dimensional, or three-dimensional grid, similarly, one thread block can also be organized into one-dimensional, two-dimensional or three-dimensional. The organization of the block and grid shape and dimension is determined by the concrete

application, Figure 1 shows the 3 dimensional thread hierarchy of CUDA. In Figure 2 we

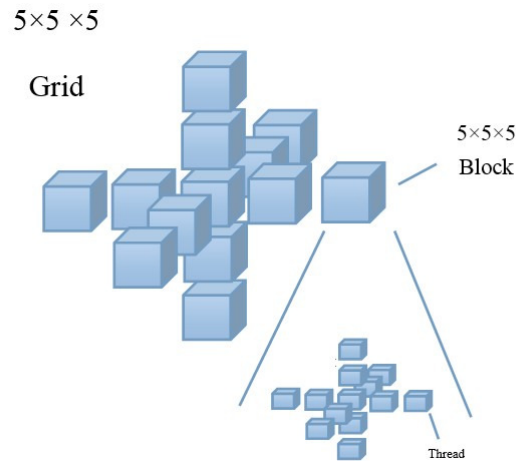


Figure 1: CUDA 3D thread hierarchy
 $5 \times 5 \times 5$ grid and each block contains $5 \times 5 \times 5$ threads

use the GPU-GeForce GTX 760 as an example to show the microarchitecture of GPU. The GPU works as a coprocessor system, consists of Stream Multiprocessors (SM), GeForce GTX 760 has 6 SM performs the multiply-add arithmetic operation and furthermore, each SM has the special functional units(SFU) that can perform more complex arithmetic operation such as trigonometric functions and reciprocal square root. the shared memory is also called on-chip memory which is located at SM that has low latency and limited capacity. Global memory, which is off-chip located memory of GPU with long latency and large capacity, another two types of the memory is called texture memory and constant memory, which are located off-chip , but cached, therefore the loading speed of the data located at these two type of memory space will be much faster than the that from global

memory, for constant memory, it is read only and the memory latency is approximately as small as the registers. The variables invoked in kernel functions can be stored in either of the these 4 types of memories. Registers are allocated dynamically to threads.

Since the resource limitation of SM the total number of threads that we can define in one block is limited, on current CUDA supported GPUs, one block can contains up to 1024 threads, in addition all the blocks are executed on SMs, thus the total number of threads we can make use of is $T_{total} = Num_{SM} \times Num_{threads/SM}$, GeForce GTX 760 allows 2048 threads in one SM, thus the total number of threads that can work in parallel is $2048 \times 6 = 12288$, although in concrete application, the programmer can allocate more than 12288 threads for a kernel, but the threads will work in serial, which will influence the performance of program.

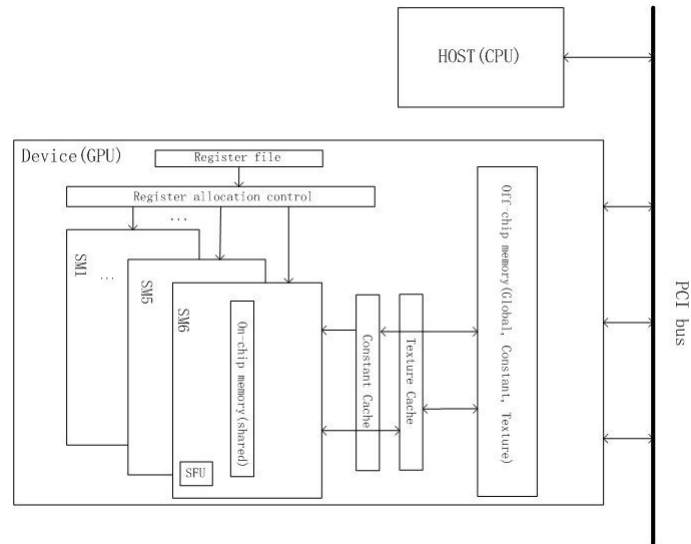


Figure 2: High View of CUDA CPU Microarchitecture

4 GPU Based Acceleration of FCSD

In this section we present the parallel implementation of fixed complexity sphere decoder

by GPU, first from (1), the maximum likelihood (ML) solution is given by:

$$s_{ML} = \arg \min_{s \in \mathbb{O}^{N_t}} \|y - \mathbf{H}s\|^2 \quad (2)$$

we consider the array $N_t = N_r$, performing QR decomposition to channel propagation matrix

$$\mathbf{H} = \mathbf{Q}\mathbf{R} \quad (3)$$

where $\mathbf{Q} \in \mathbb{C}^{N_t \times N_t}$ is the unitary matrix, $\mathbf{R} \in \mathbb{C}^{N_t \times N_t}$, is the upper triangular matrix,

the basing on [?], the (2) can be changed to

$$\begin{aligned} s_{ML} &= \arg \min_{s \in \mathbb{O}^{N_t}} \|\mathbf{Q}^H y - \mathbf{Q}^H \mathbf{H}s\|^2 \\ &= \arg \min_{s \in \mathbb{O}^{N_t}} \|\mathbf{Q}^H y - \mathbf{R}s\|^2 \end{aligned} \quad (4)$$

Consider the unconstrained estimation of s , $\hat{s} = \mathbf{G}y$, $\mathbf{G} = (\mathbf{H}^H \mathbf{H})^{-1} \mathbf{H}^H$ denotes the zero

forcing equalizer, basing on 3, we have

$$\hat{s} = \mathbf{G}y = (\mathbf{R}^H \mathbf{R})^{-1} \mathbf{R}^H \mathbf{Q}^H y = \mathbf{R}^{-1} \mathbf{Q}^H y \quad (5)$$

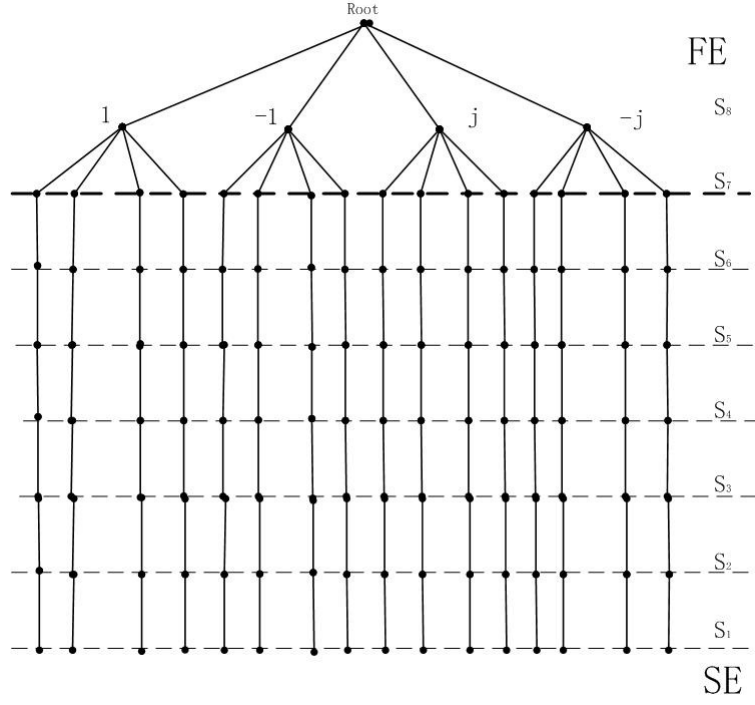


Figure 3: Tree searching of QPSK FCSD for 8x8 MIMO system

Therefore $\mathbf{Q}^H y = \mathbf{R} \hat{s}$, the 4 can be changed to

$$s_{ML} = \arg \min_{s \in \mathbb{O}^{N_t}} \|\mathbf{R}(\hat{s} - s)\|^2 \quad (6)$$

the Fixed Complexity Sphere Decoder works as a constant number of multiple path tree searching. As shown in Figure 3, just like SD the FCSD also performs depth first searching, at the first ρ level the FCSD search all the possible signal symbols $\tilde{s}_{N_t} \tilde{s}_{N_t-1} \dots \tilde{s}_{N_t-\rho+1}$ in constellation \mathbb{O}^{N_t} , which is called Full Expansion(FE) level, the remain $N_t - \rho$ levels of symbols, the FCSD performs decision feed back equalization (DFE), from (6) the solution

of FCSD can be given:

$$\hat{s}_{FCSD} = \arg \min_{s \in \mathbb{O}^{N_t}} \sum_{i=1}^{N_t} |r_{ii}(\hat{s}_i - s_i) + \sum_{j=i+1}^{N_t} r_{ij}(\hat{s}_j - s_j)|^2 \quad (7)$$

$i \in [1, 2 \dots N_t]$, r_{ij} denotes the element at the i th row and j th column of the upper triangular matrix \mathbf{R} , this process is called Single Expansion (FE). thus the FCSD solution $s_{FCSD} = [s_1, s_2 \dots s_{N_t}]$ can be expressed as:

$$s_{FCSD}^i = \begin{cases} \in \mathbb{O}^\rho & i = N_t, N_t - 1, \dots, N_t - \rho + 1 \\ \mathbb{Q}[\hat{s}_i + \sum_{j=i+1}^{N_t} \frac{r_{ij}}{r_{ii}}(\hat{s}_j - s_{FCSD}^j)] & i = N_t - \rho, N_t - \rho - 1, \dots, 2, 1 \end{cases}$$

$\mathbb{Q}[]$ denotes the signal constellation based quantization. At the post processing stage,

FCSD takes the symbol vector candidate with the minimum Euclidean metric E_{metric} :

$$E_{metric} = ||\mathbf{R}(\hat{s} - \tilde{s})||^2 \quad (8)$$

The \tilde{s} denotes the symbol vector candidate, the total number of candidates is:

$$M^\rho \quad (9)$$

4.1 CUDA-FCSD Pre-Prossing

As shown in figure.4, each path of the FCSD searching has a serial execution nature, in order to avoid error propagation of decoder, FCSD ordering was applied to the propagation channel based on post processing signal to noise ratio [?], which can be expressed as:

$$\varphi_m = \frac{E_s}{\sigma^2(\mathbf{H}^H\mathbf{H})_{mm}^{-1}} \quad (10)$$

φ_m denotes the post processing signal to noise ratio of the m th data stream, $(\mathbf{H}^H\mathbf{H})_{mm}^{-1}$ denotes the diagonal elements of the inversion of HHH matrix $\mathbf{H}^H\mathbf{H}$, thus when the SNR is determined, the post processing SNR is only determined by $(\mathbf{H}^H\mathbf{H})_{mm}^{-1}$, for the FE stage the robustness of detector performance is not influenced by the post processing SNR thus at FE stage the "weakest" data stream is detected first, that is, the data stream with the smaller φ is detected earlier. At SE stage, because of the single searching path of the symbol, the performance is tightly related to the post processing SNR, therefore at SE stage the data streams with the larger post processing SNR is detected earlier in order to avoiding the error propagation, in conclusion the FCSD ordering works iteratively and obeys the following rule: At the j th step ($j = 1, 2 \dots N_t - 1$), s_p denotes the symbol to

be detected, where

$$p = \begin{cases} \arg \max_k (\mathbf{H}_j^H \mathbf{H}_j)_{kk}^{-1} & FEstage \\ \arg \min_k (\mathbf{H}_j^H \mathbf{H}_j)_{kk}^{-1} & SEstage \end{cases}$$

$\mathbf{H}_j \in \mathbb{C}^{N_r \times (N_t - j + 1)}$ denotes the renewed channel matrix, at the j th iteration with the column corresponding to previous detected data streams removed from \mathbf{H}_{j-1} . the unconstrained estimation \hat{s} in 5 is given by:

$$\hat{s} = (\mathbf{H}^H \mathbf{H})^{-1} \mathbf{H}^H y \quad (11)$$

Although the FCSD pre-processing has a serial nature and can not be vectorized, the computational consumptive operations 4.1 11 can be implement by the CUDA Basic Linear Algebra Subprograms(cuBLAS), the matrix inverse(Gaussian Jordan Elimination) and cholesky factorization(Row Major Factorization) are also implemented by GPU, as shown in Table 1.

Table 1: Parallel Computation Operation of FCSD Pre-processing

Operations	complex matrix-matrix multiplication	complex matrix-vector multiplication	matrix inverse	cholesky factorization
GPU subroutine	<i>cublasCgemm</i>	<i>cublasCgemv</i>	<i>GJE</i>	<i>chol</i>
Formula	$\mathbf{H}^H \mathbf{H}$	$(\mathbf{H}^H \mathbf{H})^{-1} \mathbf{H}^H y$	$\mathbf{H}_j^H \mathbf{H}_j)^{-1}$	$\mathbf{H}^H \mathbf{H} = \mathbf{R}^H \mathbf{R}$

Figure 4 shows the block diagram of the CUDA-FCSD implementation, as mention in section 3, our implementation is based on heterogeneous programming principle, the flow control and logical operations are reside at the host side, the compute intensive works is implemented at device side.

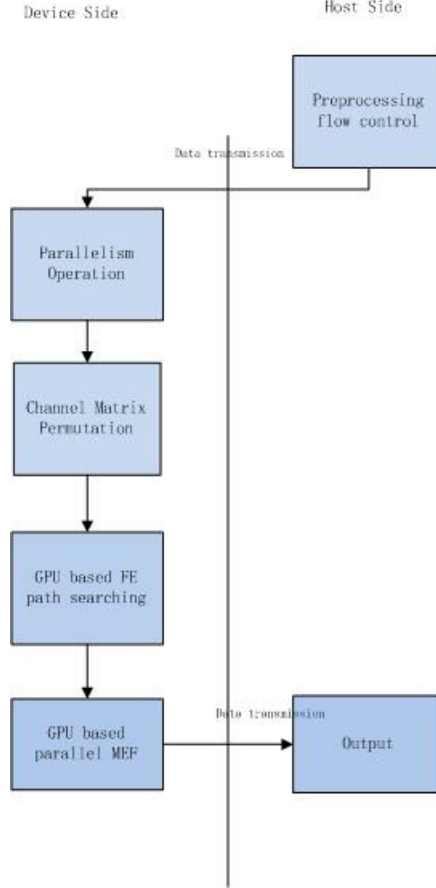


Figure 4: Block Diagram of CUDA-FCSD Implementation

4.2 Parallel Acceleration of Blocked-Paths Searching

We consider 16×16 MIMO system, the modulation scheme is 16QAM, the path we need to search is $\mathcal{O}[M^\rho] = 16^3 = 4096$, $\rho = \lceil \sqrt[3]{N_t} - 1 \rceil$, as mentioned in section 3 the maximum

number of threads that can be used in GPU is limited by the number of SM and maximum number of threads per SM, as to GeForce GTX 760. we have 12288 threads totally. For each path, decision feedback path searching has a serial nature, therefore we match path to one thread, in order to have largest amount of threads that can be paralleled, we use one dimension blocks for widest expansion and blocked all the paths into several one dimension blocks, for largest SM occupation we define 4 blocks for path searching kernel and each block has 1024 threads. At each path, we perform the following data operation:

1. *Decision Feedback Equalization*

$$\begin{aligned}
s_i^k &\in \mathbb{O}^\rho \quad \text{if } i = N_t, N_t - 1, \dots, N_t - \rho + 1 \quad FE \\
s_i^k &= \hat{s}_i^k + \sum_{j=i+1}^{N_t} \frac{r_{ij}}{r_{ii}} (\hat{s}_j^k - s_j^k) \quad \text{if } i = N_t - \rho, N_t - \rho - 1, \dots, 2, 1 \quad SE
\end{aligned} \tag{12}$$

s_j^k denotes the j th symbol of the k th symbol vector candidate.

2. *Euclidean Metric Calculation*

$$E_u^k = \sum_{i=1}^{i=N_t} \sum_{j=i}^{j=N_t} r_{ij} (\hat{s}_j - s_j) \tag{13}$$

E_u^k denotes the k th Euclidean metric of the corresponding symbol vector candidate \tilde{s}^k .

Then we take the symbol vector s^θ as the solution, where

$$\theta = \arg \min_m (E_u^m) \quad m = 1, 2 \dots M^\rho \quad (14)$$

4.2.1 Data Preparation

There are three major factors that will influence the configuration of the data set configuration in memory space.

1. Amount of Reading&Writing operation per thread.
2. Program scope of the data.
3. Storage Requirement of data.

The memory reading&writing (R/W) strategy of GPU is the crucial factor that influence the application performance because the GPU is data processing intensive and only has small cache for special memory space(constant, texture), another consideration is the validation life circle of data, local memory which is invoked in kernel function is valid in one thread, share memory is valid in one block, constant, texture and global memory are valid both at host side and device side. On the other hand different from global memory (2047 MBytes in GeForce GTX 760), the constant and share memory are all capacity limited (only 65536 bytes totally and 49152 bytes per block in GeForce GTX 760), so

that for our application the configuration of memory is determined by the capacity requirement of the data. Here in table 2 we present the amount of R/W operations and the storage that needed for critical data variables in FCSD path searching. The amount of the R/W operation is calculated based on the (12) and ((refEu metric), for complex value $(\mathbf{R}, \hat{s}, s_{potentialmatrix}, s_{kernel})$ is stored use *float2* which counts 8 bytes, floating point data set E_u is stored in *float*, which counts for 4 bytes, s_{index} is the integer list which is stored use *int*, which counts 1 byte.

At host side we set 4 vector data set that are stored linearly in global memory which has program scope for both host side and device side, $s_{potentialmatrix}$ is used to store the $M^\rho \times N_t$ complex matrix that each row stores one symbol vector candidate and whose valid scope is through the whole kernel function. s_{index} , which is used to store the index of all the possible sub symbol vectors for FE stage using full factorial method, requires a $\rho \times M^\rho$ integer matrix space. E_u is a M^ρ floating point vector that is used to store the Euclidean metric of all the symbol vector candidates, obviously the valid scope of it is for the whole kernel function. s_{kernel} is a complex vector used to store the FCSD solution which length is N_t and has to be transferred to host side, thus it is also needed to be stored in global memory.

On the other hand, upper triangular matrix \mathbf{R} in (6) and unconstrained estimation \hat{s} in (5) requires a large amount of R operations and are read only. (for the 16×16 16QAM

MIMO system the R/W of \mathbf{R} and \hat{s} are about 370 and 266 per thread), these two data set need small size of storage(for the 16×16 16QAM MIMO system 1088 bytes for \mathbf{R} and 128 bytes for \hat{s}) we make use of the read only constant memory to store the data which are capacity limited and do not need write operation in path searching , as we mentioned in section (3), the constant memory is cached so that it is much faster than global memory.

Table 2: Amount of R/W Operations and Storage Requirement of Different Data Set

data	\mathbf{R}	\hat{s}	$s_{potentialmatrix}$	s_{index}	E_u	s_{kernel}
R/W operations/thread	$(\frac{3}{2}(N_t)^2 - \frac{N_t}{2} + \rho - \rho^2)$	$(\frac{2(N_t)^2 + 2N_t - \rho^2 - \rho}{2})$	ρ	N_t	N_t	N_t
Storage/bytes	$4(N_t + 1)N_t$	$8N_t$	$8M^\rho N_t$	$N_t M^\rho$	$4N_t M^\rho$	$8N_t$

4.2.2 Memory Access Pattern

When considering large MIMO array, the large amount of R/W operations determine that the memory bandwidth is the major bottleneck of the performance, although the theoretical bandwidth of off-chip memory is extremely high (in GeForce GTX 760 the bandwidth of off-chip memory is around $192GB/s$), however the effect memory bandwidth can only be achieved by proper R/W strategy.

Global memory is implemented by dynamic random access memory (DRAM) whose R/W is extremely slow process, modern DRAM R/W data by access a pitch of consecutive

memory location, as mentioned in section (3), the warp is the basic schedule unit of device, with one instruction recall one warp of threads that execute at the same time, the most favorable global memory access pattern is to keep one warp of threads that access consecutive memory as much as possible, for GeForce GTX 760, the DRAM will access a consecutive memory address that has 128 bytes length, In Figure 5 we take the global access pattern of the $s_{potentialmatrix}$ as an example to illustrate how we coalesce the the global memory, we store $s_{potentialmatrix}$ in one pitch of linear global memory, with each row store one $N_t = 16$ complex symbol vector solution candidate of \hat{s}_{FCSD} in (7), totally there are $M^p = 4096$ rows, this matrix is stored in column major. As mentioned before we operate one path in one thread, thus the address two consecutive symbol operated in one thread is 4096, however for consecutive threads the address they reach is continues as shown in Figure 5, each 32 threads in one warp can make R/W operation to a pitch of continues memory, which is $32 \times 8 = 256bytes$, counts for two times of DRAM access. Another available resource for memory bandwidth increase is to make use of share memory, for all the transient variables that used for accumulator in (12) and (13), because of the small capacity consumption and large amount of R/W operations.

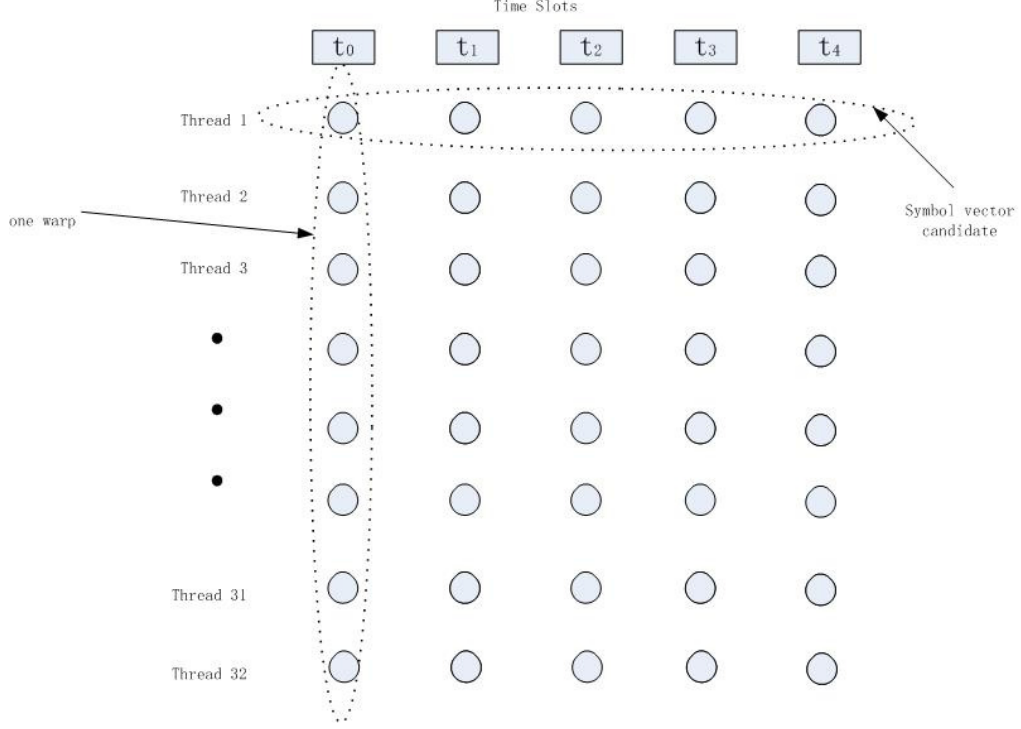


Figure 5: Global Memory Access Pattern of $s_{potentialmatrix}$

4.2.3 Data Transfer Minimization

The data transfer between the host side and the device side is much more slower than the inner device data transferring, therefore, in our application we minimize the data transferring times, we make data transfer only once for propagation channel matrix \mathbf{H} , received symbol vector y in (1) as well as the index list s_{index} at FE stage, we integrate the post processing (13) into path searching kernel function to avoid the transferring of E_u in (13).

4.3 Going to Larger MIMO System

Consider the uplink 32×32 MIMO system with 16QAM modulation scheme, from 9, the path number that need to be searched is $16^5 = 1048576$, as mentioned in section (3), the maximum number of threads that can be execute in kernel function of GeForce GTX 760 is 12288, therefore we need to consider serial the one kernel into a certain times of loop, in order to avoid device synchronization latency, we synchronize and return the control to host side in order to reduce the synchronization expense. Under this condition we use 12 linear blocks and each block has 1024 threads, we execute the kernel function for 86 times and get the final solution.

5 Simulation Results

5.1 Environment

5.1.1 Device

Graphic Processing Units: GeForce GTX 760, GPU clock rate: 1.08 GHz , memory clock rate: 3 GHz , number of SM: 6, maximum number of threads per stream multiprocessor: 2048, total amount of global memory: 2 GB, total amount of share memory per block: 49 KB, total amount of constant memory: 66 KB.

Central Processing Units-Modigliani: Intel Core i5-4th generation, 4 cores 3.20 GHz CPU

clock rate, 8 GB RAM

Central Processing Units-Monet : Intel Core i7-3rd generation, 12 cores 3.20 GHz CPU

clock rate, 32 GB RAM

5.2 Software

CUDA Driver Version / Runtime Version 6.5 / 6.0

Nsight Eclipse Version 6.5

5.3 Performance and Evaluation

Table 3: Speedup Performance of different MIMO Array size

Array size	Time/s			Speedup	
	GTX 760	modigliani	monet	GTX/modigliani	GTX/monet
8	0.46	0.09	0.08	0.20	0.17
16	1.56	3.2	3.57	2.05	2.29
20	31	74	81	2.39	2.61
25	38	112	122	2.94	3.21
32	611	2836	3033	4.64	4.96

We test 5 array sizes and make comparison between GTX 760 and two kinds of CPU, all the operation times we test is based on 100 channel realizations, the transmitted data is generated randomly and modulated by 16 QAM modulation scheme, as we can see in

3, for small size array, like 8×8 , GPU has no advantage over CPU, for small array size, the number of path that need to be searched is relatively small, the CPU has already had a good performance, there is a short time for GPU to "warm up", for data transferring, launch kernel function and host device synchronization, further more, for small number of threads, the memory R/W latency is not well hided. When the array size grows large, a large parallelism is achieved so that the GPU begin to display its data processing power, and with the array size increasing, this speedup tends to be much more considerable.

6 Conclusion

In this paper, we present the GPU implementation of fixed complexity sphere decoder for a large MIMO system, which is a time consuming task for traditional platform, we have reached up to nearly 5 times acceleration of FCSD and this speedup grows higher with the increasing array size. In addition, the GPU and CPU can work independently, the data processing power of GPU computing is an extra bonus of the traditional simulation platform. This shows the potential of GPU computing for the simulation and consumptive computational work of large MIMO area.

References

- [1] C. Oestges and B. Clerckx, *MIMO wireless communications: from real-world propagation to space-time code design*. Academic Press, 2010.
- [2] E. Dahlman, S. Parkvall, J. Skold, and P. Beming, *3G evolution: HSPA and LTE for mobile broadband*. Academic press, 2010.
- [3] F. Rusek, D. Persson, B. K. Lau, E. G. Larsson, T. L. Marzetta, O. Edfors, and F. Tufvesson, “Scaling up mimo: Opportunities and challenges with very large arrays,” *Signal Processing Magazine, IEEE*, vol. 30, no. 1, pp. 40–60, 2013.
- [4] E. G. Larsson, O. Edfors, F. Tufvesson, and T. L. Marzetta, “Massive mimo for next generation wireless systems,” *arXiv preprint arXiv:1304.6690*, 2013.
- [5] E. Viterbo and J. Boutros, “A universal lattice code decoder for fading channels,” *Information Theory, IEEE Transactions on*, vol. 45, no. 5, pp. 1639–1642, 1999.
- [6] B. Hassibi and H. Vikalo, “On the sphere-decoding algorithm i. expected complexity,” *Signal Processing, IEEE Transactions on*, vol. 53, no. 8, pp. 2806–2818, 2005.
- [7] L. G. Barbero and J. S. Thompson, “Fixing the complexity of the sphere decoder for mimo detection,” *Wireless Communications, IEEE Transactions on*, vol. 7, no. 6, pp. 2131–2142, 2008.
- [8] J. Fung and S. Mann, “Using graphics devices in reverse: Gpu-based image processing and computer vision,” in *Multimedia and Expo, 2008 IEEE International Conference on*. IEEE, 2008, pp. 9–12.
- [9] W. Blewitt, G. Ushaw, and G. Morgan, “Applicability of gpgpu computing to real-time ai solutions in games,” *Computational Intelligence and AI in Games, IEEE Transactions on*, vol. 5, no. 3, pp. 265–275, 2013.
- [10] W. J. van der Laan, A. C. Jalba, and J. B. Roerdink, “Accelerating wavelet lifting on graphics hardware using cuda,” *Parallel and Distributed Systems, IEEE Transactions on*, vol. 22, no. 1, pp. 132–146, 2011.
- [11] C. Xanthis, I. Venetis, A. Chalkias, and A. Aletras, “Mrisimul: A gpu-based parallel approach to mri simulations,” *Medical Imaging, IEEE Transactions on*, vol. 33, no. 3, pp. 607–617, March 2014.
- [12] S. Grauer-Gray, W. Killian, R. Searles, and J. Cavazos, “Accelerating financial applications on the gpu,” in *Proceedings of the 6th Workshop on General Purpose Processor Using Graphics Processing Units*. ACM, 2013, pp. 127–136.
- [13] C. Nvidia, “Programming guide,” 2008.